The Journal of Physical Chemistry B

 VOLUME 103, NUMBER 10, MARCH 11, 1999

# LETTERS

## Observations of Anisotropic Electron Scattering on Graphite with a Low-Temperature Scanning Tunneling Microscope

**J. G. Kushmerick,[†] K. F. Kelly,[‡] H.-P. Rust,[†,§] N. J. Halas,*[,‡] and P. S. Weiss*[,†]**

*Department of Chemistry, 152 Davey Laboratory, The Pennsylvania State University, University Park, Pennsylvania 16802-6300, Department of Electrical and Computer Engineering, Rice Quantum Institute, and Center for Nanoscale Science and Technology, Rice University, P.O. Box 1892, Houston, Texas 77251, and Fritz-Haber-Institut der Max-Plack-Gesellschaft, Faradayweg 4-6, 14195 Berlin, Germany*

*Received: September 9, 1998; In Final Form: January 19, 1999*

Low-temperature scanning tunneling microscopy was used to observe anisotropic (3-fold) scattering from point defects on a graphite surface. Such scattering from defects was theoretically predicted but is not typically apparent in room temperature scanning tunneling microscope images. This 3-fold scattering was previously observed only with $C_{60}$-functionalized tips. The occupancy of the density of electronic states of the tungsten probe tip is sharpened sufficiently at cryogenic temperatures to enable the electron scattering to be imaged.

### Introduction

The scanning tunneling microscope (STM) can be used to monitor local scattering and perturbations of electronic surface states, both from naturally occurring surface defects[1] (such as contaminant atoms and step edges) as well as from fabricated nanostructures.[2] These scattered electron waves can be isotropic[1] or anisotropic[3] depending on the scatterer and the symmetry of the crystal face investigated. The roles that scattered surface states play in directing molecular adsorption[4] and enhancing catalytic rates[5] have been investigated. Here we report the observation of anisotropic scattering from point defects in a graphite surface with the metal probe tip of a low-temperature STM.

This anisotropic scattering is consistent with theoretical predictions made by Mizes and Foster[6] and extended by Kelly and Halas[7] for scattering from point defects on graphite. The images are also in agreement with previously reported observations of 3-fold scattering using a $C_{60}$-functionalized probe tip at room temperature.[8] The ability to observe this anisotropic scattering with a metal tip only at low temperatures is consistent with the proposed resolution enhancement found for $C_{60}$-functionalized tips. A narrow distribution of tip electronic states, whether molecular orbitals of a $C_{60}$-functionalized tip or the cryogenically sharpened Fermi distribution of a metal tip, appears to be necessary to image the anisotropic electronic perturbations.

### Experimental Section

All experiments were performed in a low-temperature ultra-high-vacuum (UHV) STM operated at 77 K, which has been described previously.[9] Briefly, three room-temperature UHV chambers contain the surface preparation and analysis tools. A connected low-temperature stage contains a beetle-style STM, with multiple layers of vibration isolation separating the microscope from the surrounding environment.

The STM tips were prepared by mechanically cutting polycrystalline W wire. Tips were examined using an optical microscope, and any tips that were shattered or appeared to have unfavorable geometries were discarded. Tips so prepared readily yielded atomic resolution of the HOPG surface and 3-fold

[†] The Pennsylvania State University.
[‡] Rice University.
[§] Fritz-Haber-Institut der Max-Plack-Gesellschaft.

10.1021/jp983648v CCC: $18.00 
Published on Web 02/20/1999

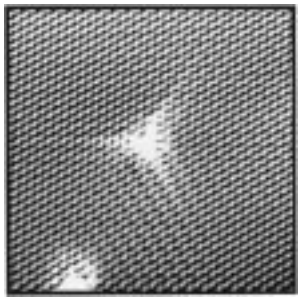

**Figure 1.** Atomic resolution STM image of anisotropic electron scattering from a point defect on highly oriented pyrolytic graphite (75 Å × 75 Å image area, sample bias = 50 mV, tunneling current = 500 pA, temperature = 77 K).

scattering from point defects. Once inserted into the UHV system, we have no means of replacing the tip, thus in situ tip regeneration is paramount. Upon accidental tip−sample contact, the tunnel junction often became unstable. By scanning at large gap impedances (e.g., 50 pA at 3V), a stable tip could be created, which once again was capable of imaging the lattice and defect scattering. Alternatively, as sample exchange is possible in our STM, the probe tip could be brought into contact with a metal substrate or could be cleaned and sharpened via field emission.[10] Although the tips are nominally W, the chemical identity of the outermost atomic asperity is unknown.

The highly ordered pyrolytic graphite (HOPG) samples were prepared by cleaving in air with adhesive tape followed by gentle resistive heating in the UHV system to remove surface contaminants. Single-atom surface vacancies (point defects) can be formed by sputtering a graphite surface with argon ions;[11,12] however, a small number are present naturally on unsputtered surfaces, and these are the focus of this study. Point defects were located by imaging relatively large areas of the HOPG surface (e.g., 5000 Å × 5000 Å), followed by higher resolution scans of suspected defects. Defects exhibiting anisotropic scattering had an average density of greater than 1 per 2000 Å × 2000 Å area and were randomly distributed (total point defect densities were typically 1 per 1000 Å x 1000 Å area). No evidence of clustering or defect−defect repulsion could be inferred.

All images were acquired in constant current mode with the bias voltage applied to the sample relative to the tip and are shown here unfiltered. Images of defect-free areas of the graphite surface exhibited the trigonal symmetry and lattice spacing of the $\beta$-site sublattice,[13] which is exclusively imaged at the low-bias voltages used in this study.[14]

## Results and Discussion

Figure 1 is a representative atomic-resolution STM image of anisotropic electron scattering from a point defect on a graphite surface obtained with a W metal probe tip. The scattering pattern is in excellent agreement with both the theoretical predictions and the previously reported 3-fold scattering observed with $C_{60}$-modified tips. The $\beta$-site carbon lattice as well as the 3-fold symmetric scattering "arms" of the point defect are resolved. In the lower left corner of the image, a second defect or adsorbate not exhibiting 3-fold scattering is also found. Anisotropic scattering from point defects was observed with both positive and negative sample biases over a small bias window, which is discussed in greater detail below.

The original simulation by Mizes and Foster predicting 3-fold scattering[6] used a single graphite sheet to model the HOPG surface and only considered contributions from $\beta$-site carbon

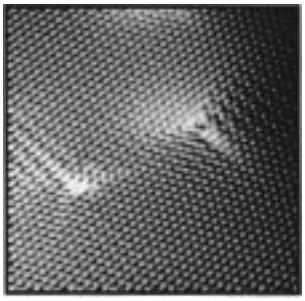

**Figure 2.** STM image showing one α-site and $\beta$-site point defect on highly oriented pyrolytic graphite exhibiting anisotropic electron scattering. The two measured electronic perturbations are rotated 60° with respect to one another due to their different local geometry (75 Å x 75 Å image area, sample bias = 50 mV, tunneling current = 750 pA, temperature = 77 K).

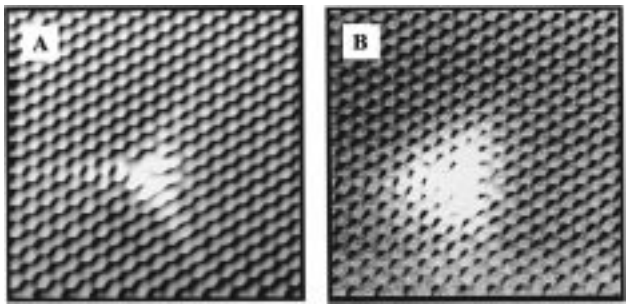


**Figure 3.** Two images of a single point defect on highly oriented pyrolytic graphite acquired at sample biases of (A) −50 and (B) −100 mV. With the larger magnitude bias voltage, the anisotropic nature of the perturbation is reduced (for both images 40 Å x 40 Å image area, tunneling current 1 nA, temperature = 77 K).

atoms. The α-site carbon energy levels are far from the Fermi level,[14] and thus they were assumed not to contribute to the low-voltage STM images. This assumption led directly to the conclusion that only defects at $\beta$-sites would exhibit 3-fold scattering. Kelly and Halas used a more complete cluster bilayer model, including contributions from both α-sites and $\beta$-sites and both predicted and observed 3-fold scattering from defects at both sites.[7] The scattering superlattice structure differs for point defects depending upon their location in the graphite lattice, thus facilitating determination of the defect site position. The most prominent difference between the two types of point defects is that they scatter electrons along different crystallographic directions. Defects at α-sites ($\beta$-sites) scatter electrons along the rows of the $\beta$-site (α-site) sublattice, which was originally predicted by Soto.[15] Figure 2 is an STM image of two point defects exhibiting anisotropic scattering. The perturbations due to the two defects are rotated 60° with respect to one another and thus are taken to be examples of α-site and $\beta$-site defects. The assignment of the defect position can be obtained by comparing the theoretical model with careful Fourier space lattice−superlattice filtering analysis of the experimentalSTM image.[7] The results of this analysis indicate that the defect on the left is located at an α-site and that the right defect is located at a $\beta$-site.

The question of why these defects are observable with a metal tip at cryogenic temperature, but not at room temperature, remains. Two atomic-resolution STM images of a single defect acquired at two different bias voltages are shown in Figure 3. The image acquired at −50 mV (Figure 3a) exhibits anisotropic electron scattering. Changing the applied bias voltage to −100 mV (Figure 3b) dramatically changes the image characteristics. The scattering arms are no longer resolved, although some of the 3-fold symmetry remains. As the bias voltage is further

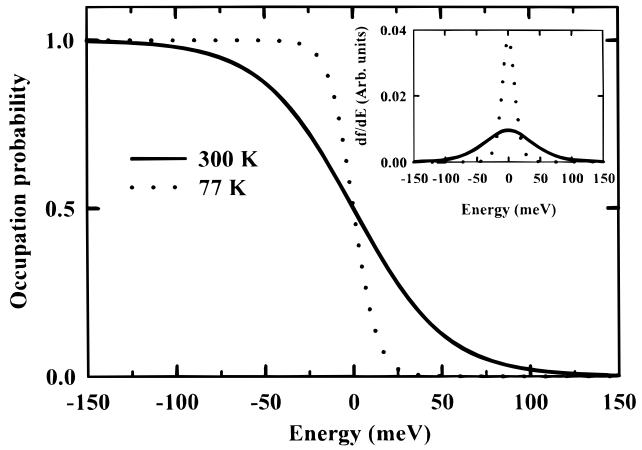


**Figure 4.** Fermi distributions of electron occupation in a metal at 300 (solid line) and 77 K (dotted line). Inset is a plot of d$f$/d$E$ vs $E$ showing the effect of temperature on the energy broadening of the electron distribution. The energy scales for the graphs are relative to the Fermi level of the metal. The occupancy of the density of states about the Fermi level is sharpened at 77 K, and the full-width-at-half-maximum of the energy broadening is reduced to 23 meV from 91 meV at 300 K.

increased, the defect loses even more of its long-range scattering and becomes more isotropic. The anisotropic 3-fold character of the defect is observable only over a very small voltage (energy) window.

The bias-dependent characteristics of the STM images depend on the electronic states of the defect which for some types of defects, such as vacancies, lie very close to the Fermi energy of the graphite.[15,16] As the bias voltage is shifted away from resonance with the defect states, the intensity of the scattered wave is reduced relative to the underlying lattice. As a result, the electronic perturbation surrounding the defect appears more isotropic. However, the structure of the scattered wave is strongly correlated with the Fermi surface of graphite and remains trigonally symmetric. An analogous situation is seen for the scattered electron waves on the (111) surface of noble metals and the $(10\bar{1}0)$ surface of beryllium, which remain spherically and elliptically symmetric, respectively.[17,18]

To understand the inability to observe such anisotropic scattering at room temperature with a metal tip, it is useful to consider the electron distribution of the metal probe tip. The electron distribution as a function of temperature and energy is given by the Fermi distribution function

$$f(E,T) = \frac{1}{e^{(E-\mu)/kT} + 1}$$

where $\mu$ is the Fermi energy and $k$ is Boltzmann's constant. Figure 4 is a plot of the Fermi distribution function for electrons in a metal at 300 and 77 K. The electron distribution about the Fermi level is sharpened at 77 K relative to that at room temperature (300 K). As shown in the inset to Figure 4, the full-width-at-half-maximum (FWHM) of the energy broadening due to thermally excited electrons scales as $\sim 3.5kT$, yielding a FWHM of 23 meV at 77 K and 91 meV at 300 K. It is the increased energy broadening and associated decreased energy resolution at room temperature that precludes observation of the anisotropic scattering with a metal tip. Thermally excited tip electrons tunnel into higher energy sample states, which due to their isotropic character, mask the anisotropic nature of the defect sites.[19] Thus, the loss of resolution at higher bias voltages and the inability to observe anisotropic scattering at room temperature with a metal tip are both the result of higher-energy isotropic states associated with the graphite surface. A more thorough quantitative understanding of this phenomenon would be obtained by including the tip−sample interaction at low bias voltages and differences in the tunneling matrix element (orbital overlap) between the tip and the graphite surface.

We conclude that the image characteristic's critical dependence on bias is the reason earlier studies of defects and adsorbates on graphite surfaces with metallic probe tips were unable to observe anisotropic scattering.[20] The previous studies were performed at room temperature, where there is significant thermal broadening of the density of states about the Fermi level of the STM tip. However, working at cryogenic temperatures sharpens the occupancy of the tip density of states about the Fermi level, thus enabling observation of the electron scattering. This is consistent with the interpretation of how a $C_{60}$-functionalized tip is able to resolve these electronic perturbations.[8] In both cases, a narrow energy distribution of accessible tip electronic states enables the resolution of long-range electronic scattering effects on this surface.

## Conclusions

We report observations of long-range, anisotropic electron scattering from point defects on a graphite surface with a metal tip at 77 K. The observed scattering is in close agreement with both theoretical predictions and previous observations with $C_{60}$-functionalized tips. Cryogenic temperatures narrow the occupancy of the probe tip density of electronic states about the Fermi level, thus enabling imaging of the anisotropic perturbations of the local graphite surface electronic structure.

**Acknowledgment.** The authors thank Dr. Jim Gimzewski for his comments and suggestions concerning the observation of this effect at low temperatures and Prof. Peter Nordlander for helpful discussions. The support of the National Science Foundation, the Office of Naval Research, the Petroleum Research Foundation, administered by the American Chemical Society (J.G.K., H.P.R., and P.S.W.), the Texas Advanced Technology Program (K.F.K. and N.J.H.), the Alfred P. Sloan Foundation (P.S.W.), and the Robert A. Welch Foundation (K.F.K. and N.J.H.) are gratefully acknowledged.

## References and Notes

(1) Crommie, M. F.; Lutz, C. P.; Eigler, D. M. *Nature* **1993**, *363*, 524−527. Avouris, P.; Lyo, I.-W.; Walkup, R. E.; Hasegawa, Y. *J. Vac. Sci. Technol. B* **1994**, *12*, 1447−1455. Avouris, P.; Lyo, I.-W.; Molinàs-Mata, P. *Chem. Phys. Lett.* **1995**, *240*, 423−428.

(2) Crommie, M. F.; Lutz, C. P.; Eigler, D. M. *Science* **1993**, *262*, 218−220. Heller, E. J.; Crommie, M. F.; Lutz, C. P.; Eigler, D. M. *Nature* **1994**, *369*, 464−466.

(3) Briner, B. G.; Hoffman, P.; Doering, M.; Rust, H.-P.; Plummer, E. W.; Bradshaw, A. M. *Europhys. Lett.* **1997**, *39*, 67−72. Peterson, L.; Sprunger, P. T.; Hoffman, P.; Lægsgaard, E.; Briner, B. G.; Doering, M.; Rust, H.-P.; Bradshaw, A. M.; Besenbacher, F.; Plummer, E. W. *Phys. Rev. B* **1998**, *57*, R6858−R6861.

(4) Kamna, M. M.; Stranick, S. J.; Weiss, P. S. *Science* **1996**, *274*, 118−119.

(5) Weiss, P. S.; Kamna, M. M.; Graham, T. M.; Stranick, S. J. *Langmuir* **1998**, *14*, 1284−1289. Kamna, M. M.; Graham, T. M.; Weiss, P. S. Submitted for publication.

(6) Mizes, H. A.; Foster, J. S. *Science* **1989**, *244*, 559−562.

(7) Kelly, K. F.; Halas, N. J. *Surf. Sci.* **1998**, *416*, L1085−L1089.

(8) Kelly, K. F.; Sarkar, D.; Hale, G. D.; Oldenburg, S. J.; Halas, N. J. *Science* **1996**, *273*, 1371−1373.

(9) Ferris, J. H.; Kushmerick, J. G.; Johnson, J. A.; Youngquist, M. G. Y.; Kessinger, R. B.; Kingsbury, H. W.; Weiss, P. S. *Rev. Sci. Instrum.* **1998**, *69*, 2691−2695.

(10) Meyer, J. A.; Stranick, S. J.; Wang, J. B.; Weiss, P. S. *Ultramicroscopy* **1992**, *42*−*44*, 1538−1541.

(11) Kelly, K. F.; Sarkar, D.; Prato, S.; Hale, G. D.; Halas, N. J. *J. Vac. Sci. Technol. B* **1996**, *14*, 593−596.
(12) Nordlund, K.; Keinonen, J.; Mattila, T. *Phys. Rev. Lett.* **1996**, *77*, 699−702.
(13) Graphite has two inequivalent sites for surface carbon atoms: α-site carbon atoms, centered over carbon atoms in the second layer, and *β*-site carbon atoms, centered above hollows in the second layer.
(14) Tománek, D.; Louie, S. G.; Mamin, H. J.; Abraham, D. W.; Thomson, R. E.; Ganz, E.; Clarke, J. *Phys. Rev. B* **1987**, *35*, 7790−7793. Gwo, S.; Shih, C. K. *Phys. Rev. B* **1993**, *47*, 13059−13062.
(15) Soto, M. R. *J. Microsc.* **1988**, *152*, 779−788.
(16) Mizes, H. A. Ph.D. Thesis, Stanford University, 1988.
(17) Peterson, L.; Laitenberger, P.; Lægsgaard, E.; Besenbacher, F. *Phys. Rev. B* **1998**, *58*, 7361−7366.
(18) Briner, B. G.; Hoffman, Ph.; Doering, M.; Rust, H.-P.; Plummer, E. W.; Bradshaw, A. M. *Phys. Rev. B* **1998**, *58*, 13931−13943.
(19) An analogous argument in terms of hole tunneling can explain the observation of anisotropic scattering at low negative sample bias voltages.
(20) Xhie, J.; Sattler, K.; Müller, U.; Venkateswaran, N.; Raina, G. *Phys. Rev. B* **1991**, *43*, 8917−8923. Shedd, G. M.; Russell, P. E. *J. Vac. Sci. Technol. A* **1991**, *9*, 1261. Shedd, G. M.; Russell, P. E. *Surf. Sci.* **1992**, *266*, 259−264.